Solid State Ionics 331 (2019) 66–73

Contents lists available at ScienceDirect

Solid State Ionics

journal homepage: www.elsevier.com/locate/ssi

Effect of electrostatic spray deposited nafion coating on non-lithiated LiV_3O_8 cathode in lithium-metal rechargeable batteries

Ki Yoon Bae[a], Min-woo Kim[b], Byung Hyuk Kim[a], Sung Ho Cho[a], Sam S. Yoon[b], Woo Young Yoon[a,*]

[a] Department of Materials Science and Engineering, Korea University, 1, 5Ga Anam-dong, Sungbuk-gu, Seoul 136-701, Republic of Korea
[b] Department of Mechanical Engineering, Korea University, 1, 5Ga Anam-dong, Sungbuk-gu, Seoul 136-701, Republic of Korea

ARTICLE INFO

Keywords:
Lithium metal battery
Non-lithiated cathode
Lithium trivanadate
Nafion
Electrostatic spray deposition

ABSTRACT

The effect of inert coating materials such as Nafion on the non-lithiated LiV_3O_8 cathode of lithium-metal rechargeable batteries was studied. This uniform and thin coating layer was deposited using electrostatic spray deposition to suppress the crack formation caused by volume expansion and prevent the dissolution of vanadium in the electrolyte. The Nafion coated LiV_3O_8 electrode exhibited a higher discharge capacity and better capacity retention after 200 cycles (150.86 mAh g^{-1} and 62.9%, respectively) than the bare LiV_3O_8 electrode (113.31 mAh g^{-1} and 46.8%, respectively). The Nafion coated LiV_3O_8 electrode was characterized by X-ray diffraction, Fourier-transform infrared spectroscopy, scanning electron microscopy, energy dispersive X-ray spectroscopy, transmission electron microscopy, and inductively coupled plasma mass spectrometry. Its electrochemical performance was analyzed using a battery testing system and impedance spectroscopy. Our findings show that the inert coating layer on the LiV_3O_8 cathode plays an important role in improving its electrochemical performance.

1. Introduction

Lithium-metal batteries which use lithium metal as the direct anode, have attracted interest in the electric vehicle and energy storage system industries because they provide sufficient capacity and energy density to meet the industry requirements [1,2]. Lithium metal has a higher capacity and lower potential than graphite, which is widely used at present. A recent study has reported that the use of powdered lithium metal improves electrochemical performance [3–9]. In this case, a non-lithiated cathode should be used as the counter electrode. LiV_3O_8, air, and S are the candidate materials for this electrode. Although Li–air and Li–S batteries have large capacities, they suffer from certain drawbacks. For example, Li–air batteries require oxygen for operation and show irreversible capacity initially. Further, the presence of polysulfide negatively affects Li–S batteries [10–14]. In addition, there are many material and cell-design problems; therefore, considerable research on these batteries is needed before their commercialization.

As a result, LiV_3O_8, which can be commercially applied in battery systems by making small modifications to the existing manufacturing processes, is a promising non-lithiated cathode material for lithium-metal rechargeable batteries. LiV_3O_8 offers many advantages such as low cost, easy preparation, stable layered structure, and high energy density. However, it suffers from some serious drawbacks such as a vanadium dissolution into the electrolyte, cracks caused by volumetric expansion, and low electronic/ionic conductivity [15,16], which result in capacity fading during cycling. Many methods have been proposed to resolve these issues, such as coating with polymers or metal oxides, fabricating a structure with high electronic/ionic conductivity, and doping [17–21]. Among the typical LiV_3O_8 coating materials, polyaniline, which suppresses vanadium dissolution and improves electrical conductivity [22], and aluminum oxide (Al_2O_3), which limits the irreversible phase transformation that causes volume expansion and blocks direct contact between the electrode and the electrolyte [23], have been found to be especially effective.

An inert protective layer coated on LiV_3O_8 should prevent the reaction between the electrolyte and the electrode and suppress the crack formation caused by volume expansion, thus leading to a long life cycle and high capacity. Nafion is a good inert coating material candidate because of its good cation exchange property, high ionic conductivity, and excellent stability capable of withstanding volume expansion

Abbreviations: XRD, X-ray diffraction; FT-IR, Fourier transform infrared; FE-SEM, field emission scanning electron microscopy; EDX, energy-dispersive X-ray spectroscopy; TEM, transmission electron microscopy; ICP-MS, Inductively coupled plasma mass spectrometry

* Corresponding author.
E-mail address: wyyoon@korea.ac.kr (W.Y. Yoon).

https://doi.org/10.1016/j.ssi.2018.12.020
Received 2 May 2018; Received in revised form 30 November 2018; Accepted 30 December 2018

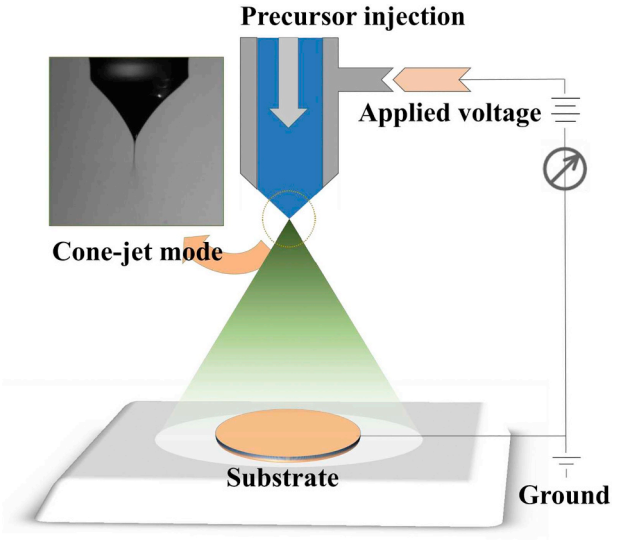

Fig. 1. Schematic of electrostatic spray deposition method.

[24–29].

A proper coating method is also very important to guarantee a uniform and homogeneous coating layer on porous materials. Therefore, electrostatic spray deposition is selected, as this method is simple and suitable for producing a uniform and fine film at the nanoscale level [30–32]. The structure, morphology, and electrochemical performance of the Nafion coated LiV_3O_8 electrode were investigated to evaluate the effectiveness of the method. This coating layer acted not only as a protective layer between the electrode and the electrolyte but also as a buffer layer against volume expansion. Therefore, it is expected that coating the LiV_3O_8 cathode with an inert material (Nafion) using electrostatic spray deposition is quite promising for enhancing the electrochemical performance of the cathode by preventing vanadium dissolution and enhancing structural stability.

2. Experimental

LiV_3O_8 was synthesized by a solid-state method using lithium hydroxide monohydrate ($LiOH{\cdot}H_2O$) and ammonium metavanadate (NH_4VO_3). First, LiOH and NH_4VO_3 were mixed using a wet milling process in a planetary ball mill, and the obtained powders were dried in a dry room for 24 h. Then, the ball-milled LiV_3O_8 precursors were ground using an agate mortar and pestle for 1 h. The precursor was transferred to a box furnace and heated at 500 °C for 12 h in air. The cathode was fabricated by casting a slurry containing the active material (LiV_3O_8, 80 wt%), a conductive material (Ketjen black, 15 wt%), and a binder material (carboxymethyl cellulose, 5 wt%) onto an aluminum foil. This electrode was dried at 70 °C for 12 h in a convection oven. After drying, Nafion ($C_7HF_{13}O_5S{\cdot}C_2F_4$) was coated on the LiV_3O_8 electrode using the electrostatic spray deposition method shown in Fig. 1. In this method, Nafion was dissolved in alcohol and water in a 1:20 M ratio of coating material to solvent. Then, the solution was introduced into a syringe pump, and a pump voltage of about 14.7 kV was applied during the coating process. The coating process lasted 3 s at a rate of 120 μL/h, and the distance of the nozzle from the LiV_3O_8 electrode was 4.5 cm. This method was the most attractive because it produced extremely fine (nanosized), self-dispersive (non-aggregating), highly wettable (electrowetting), and adhesive droplets and yielded a uniform coating layer on the electrode [30–32].

Lithium metal was used as the anode to analyze the characteristics of the bare and Nafion coated LiV_3O_8 electrodes. However, dendrite formation occurred when lithium was used in the form of a foil, which reduced the cycling efficiency and caused safety issues. Hence, lithium metal was used in the powder form, produced by the droplet emulsion technique [3–9]. This Li powder suppressed dendrite formation owing to its large surface area and low internal resistance. The Li powder was used to fabricate the electrode as follows: the as-synthesized Li powder was passed through a 20 μm sieve. Then, the sub-20-μm Li powder was stacked on a stainless steel current collector placed in a mold. A pressure of 15 MPa was applied to the mold. After pressing, a Li-powder anode was obtained.

X-ray diffraction (XRD, Rigaku SmartLab) performed using filtered Cu-Kα radiation in the 2θ range 10°–80° and Fourier transform infrared (FT-IR, HORIBA LabRam ARAMIS IR2) spectroscopy were employed to demonstrate the synthesis of LiV_3O_8 and the formation of the coating layer within 600 cm^{-1} to 2000 cm^{-1} range. In addition, the morphologies and distributions of LiV_3O_8 and the coating layer were observed using field emission scanning electron microscopy (FE-SEM, FEI Quanta 250 FEG) and energy-dispersive X-ray spectroscopy (EDX). Also, the coating layer on the LiV_3O_8 electrode was identified using high-resolution transmission electron microscopy (TEM, FEI Tecnai F20 G2) equipped with an EDX analyzer. Inductively coupled plasma mass spectrometry (ICP-MS) was employed to measure the amount of

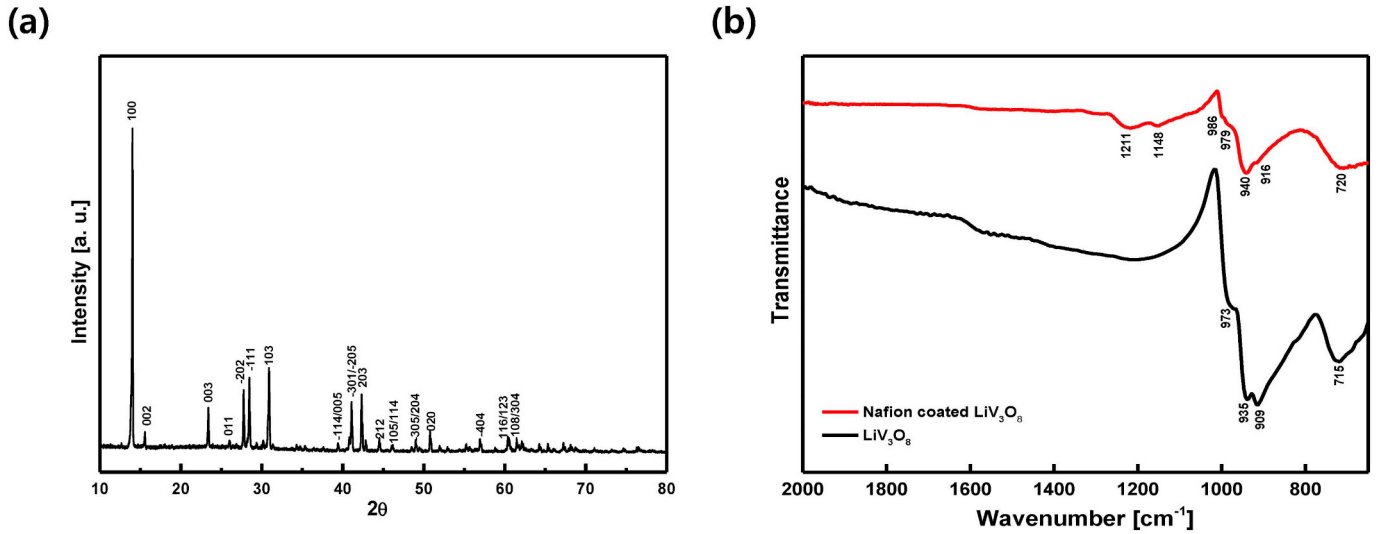

Fig. 2. (a) XRD patterns of LiV_3O_8 electrode synthesized by a solid-state method at 500 °C and (b) FTIR spectra of bare and Nafion coated LiV_3O_8 electrodes.

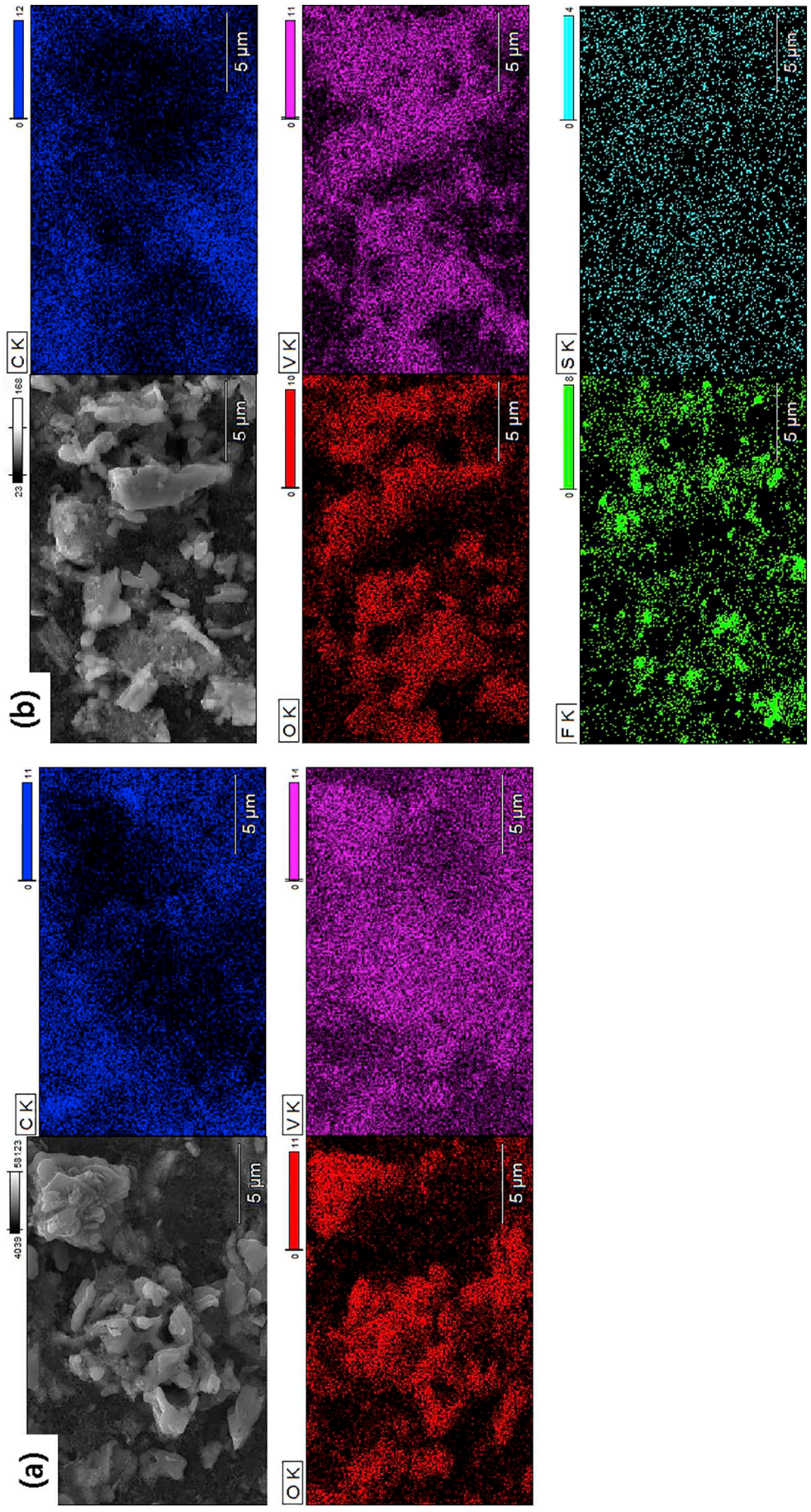

Fig. 3. EDX elemental analysis of (a) bare LiV_3O_8 and (b) Nafion coated LiV_3O_8 electrodes.

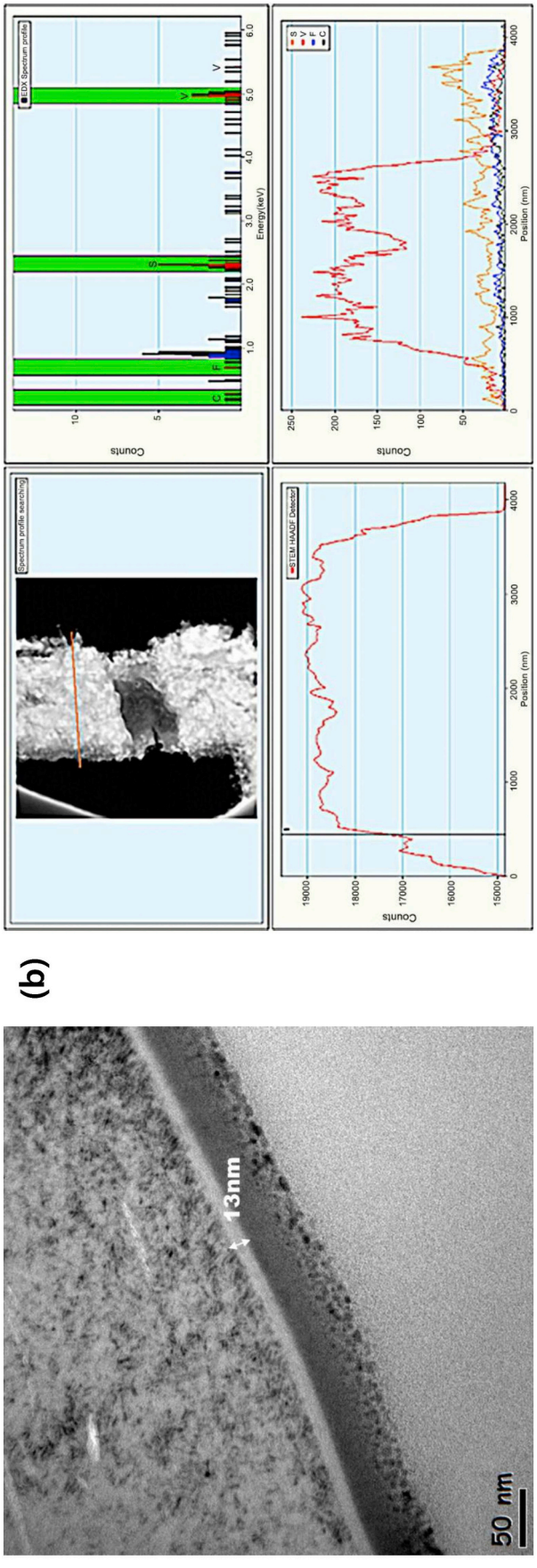

Fig. 4. (a) TEM micrographs and (b) line profiles of Nafion coated LiV_3O_8 electrode.

vanadium dissolved in the electrolyte.

The Nafion coated LiV_3O_8 electrode and the Li-powder electrode were assembled into a coin-type cell (CR2032) in a dry room. A polypropylene film (Celgard 2500) was used as the separator; 1 M $LiPF_6$ in ethylene carbonate, dimethyl carbonate, and ethyl methyl carbonate (1:1:1 volume ratio) was used as the electrolyte. Each cell was aged for 24 h after assembly in a thermostat machine, and their performance was investigated by conducting galvanostatic charge–discharge tests at 25 °C and a current density of 0.2C at 1.8–4.0 V (versus Li^+/Li) for 200 cycles using a battery testing system (WBVCS 3000, Wonatech, Korea). Electrochemical impedance spectroscopy (Solartron SI1280B, AT Frontier, Korea) was performed at frequencies ranging from 10^{-2} to 10^5 Hz at 5 mV·s^{-1}. The impedance data were processed using the software Zview (Scribner Associates Inc., Southern Pines, NC, USA) and fitted to an electrical equivalent circuit.

3. Results and discussion

Fig. 2(a) shows the XRD patterns of the bare LiV_3O_8 cathode synthesized by the solid-state method at 500 °C. The characteristic peaks of LiV_3O_8 could be indexed to monoclinic LiV_3O_8 with the space group $P2_1/m$ (JCPDS card no. 72-1193). The results indicated no impurity phase during the synthesis and a good crystallinity [33–35]. Fig. 2(b) shows the FTIR spectra for the bare and Nafion coated LiV_3O_8 electrodes. Three peaks at 909, 935, and 973 cm^{-1} could be attributed to three short V═O bonds in the LiV_3O_8 crystal and the peak at 715 cm^{-1} was attributed to the v(V−O−V) vibration of LiV_3O_8 due to the motion of the corner-sharing oxygen atom among the VO_6 and VO_5 polyhedra and Li^+. Both electrodes displayed similar peaks but those of the Nafion coated LiV_3O_8 electrode showed slight shifts. The blue shift observed for the coated LiV_3O_8 electrode confirmed the interactions among the lithium ions, Nafion molecules, and $V_3O_8^-$ layers. This could be related to the decreased interaction between the lithium ions in the interlayer and $V_3O_8^-$ and the increased interaction between the lithium ions and the Nafion molecules [36–38]. The Nafion coated LiV_3O_8 electrode was identified by the presence of peaks at 1211 cm^{-1}, corresponding to the CF_2 main-chain bonds, and 986 and 1148 cm^{-1}, corresponding to the C−F and S−O bonds, respectively. Nafion was observed to form a uniform coating layer on the surface of the LiV_3O_8 electrode.

FE-SEM equipped with EDX was performed to determine the elemental compositions of V, O, and C—the main elements of the bare and Nafion coated LiV_3O_8 electrodes. The distributions of V and O were similar to each other but were different from that of C (Fig. 3). After the coating process, F and S were uniformly distributed on the LiV_3O_8 electrode owing to the presence of Nafion [17,39]. TEM micrographs and EDX line profiles of the Nafion coated LiV_3O_8 electrode are shown in Fig. 4. TEM line profiling was performed to distinguish the S present in the Nafion coating of the conductive material. The line profile of the Nafion coated LiV_3O_8 was verified to be V in the core and S in the shell part where coating was performed. Especially, the results showed that the amount of S on the surface was larger than that below the surface, implying that Nafion was well coated on the LiV_3O_8 electrode. The thickness of the Nafion coating was about 13 nm, sufficient to interfere with Li^+ insertion/extraction and the coating layer was well formed uniformly. The SEM and TEM with EDX mapping results showed that Nafion was uniformly and thoroughly coated on the surface of the LiV_3O_8 electrode [16,23].

Fig. 5(a) and (b) show the voltage profiles of the LiV_3O_8 and Nafion coated LiV_3O_8 electrode in the 1st, 100th, and 200th cycles. Two distinct discharge plateaus were observed at 2.82 and 2.58 V. The 2.82 V discharge plateau corresponded to the insertion of the lithium ions into the empty tetrahedral sites, representing a single-phase reaction, and the 2.58 V plateau corresponded to the additional insertion of lithium ions into the tetrahedral sites, which led to a two-phase transition from $Li_3V_3O_8$ to $Li_4V_3O_8$. [16,17,35]. Note that when the charge–discharge process continued for 200 cycles, the two discharge plateaus were well

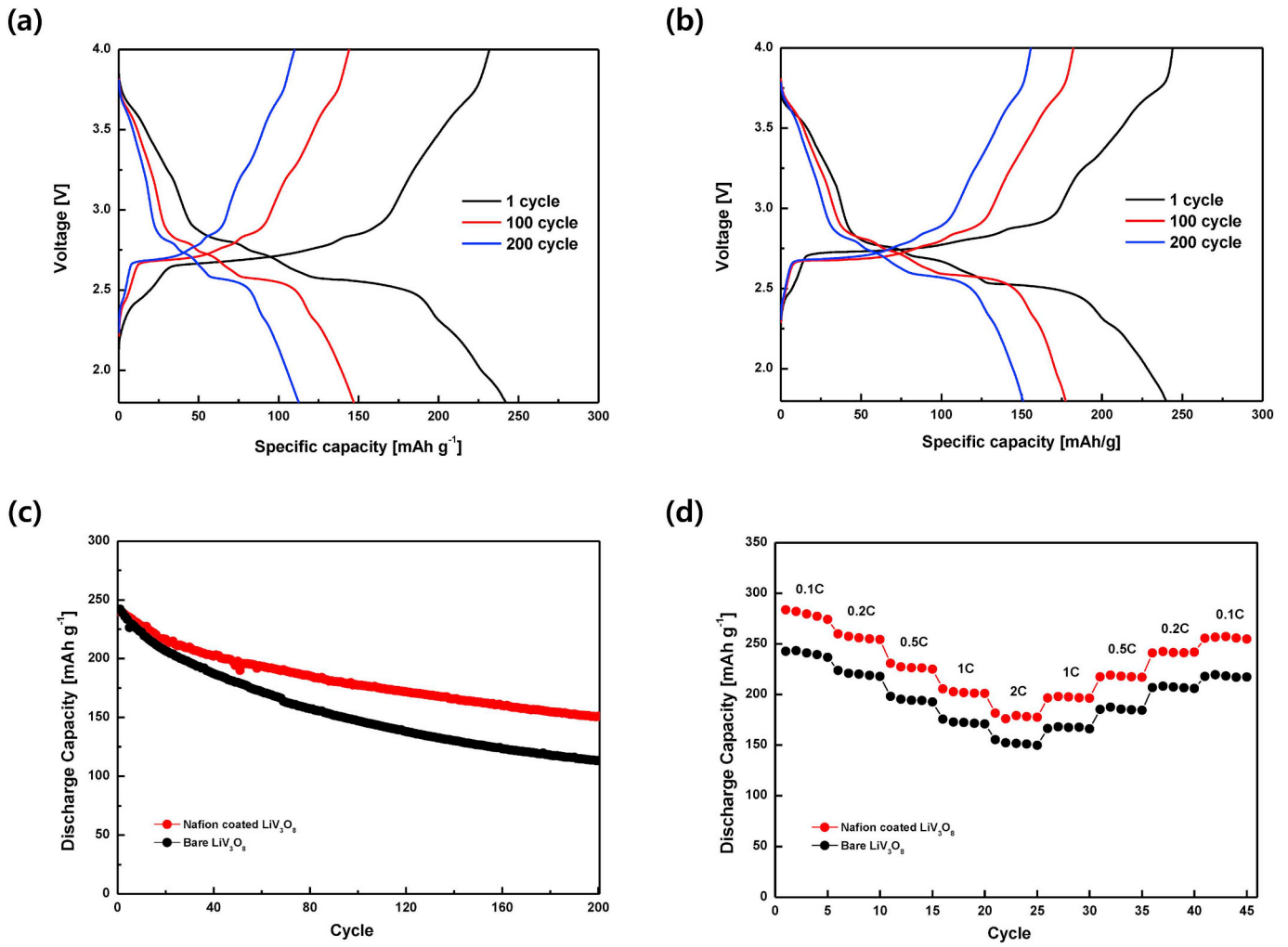

Fig. 5. Voltage profiles of (a) LiV_3O_8 and (b) Nafion coated LiV_3O_8 electrodes. (c) Cycling performance of bare and Nafion coated LiV_3O_8 electrodes at 0.2C and (d) rate capability of bare and Nafion coated LiV_3O_8 electrodes over diverse C rates.

Table 1
1st, 100th, and 200th cycle discharge capacities and retention rates of bare and Nafion coated LiV_3O_8 electrodes.

	Bare LiV_3O_8	Nafion coated LiV_3O_8
1st	242.11 mAh g^{-1}	239.84 mAh g^{-1}
100th (retention)	147.10 mAh g^{-1} (60.7%)	177.46 mAh g^{-1} (73.9%)
200th (retention)	113.31 mAh g^{-1} (46.8%)	150.86 mAh g^{-1} (62.9%)

maintained, suggesting the good stability of the crystalline structure of the Nafion coated LiV_3O_8 electrode. Fig. 5(c) and (d) show the cycling performance and rate capability of the bare and Nafion coated LiV_3O_8 electrodes, respectively. Table 1 lists the discharge capacities and retention rates in the 1st, 100th, and 200th cycles. The Nafion coated LiV_3O_8 electrode exhibited a reduced discharge capacity degradation and higher capacity retention than the bare LiV_3O_8 electrode as the number of cycles increased. Also, the coated LiV_3O_8 electrode showed a better rate capability. The charge–discharge performance of the coated electrode was more efficient at high current densities and was more stable on return to low current densities. This improved electrochemical performance was due to the uniform and nanosized coating layer achieved by electrostatic spray deposition. Thus, electrostatic spray deposition was an effective coating technique, and this Nafion coating layer induced uniform Li^+ transmission between the electrode surface and the electrolyte and suppressed current localization on the surface.

SEM images were analyzed to investigate the variations in the surface morphology of the bare and Nafion coated LiV_3O_8 electrodes after the 1st, 100th, and 200th cycles (Fig. 6). Cracks due to volume expansion of the LiV_3O_8 electrode appeared as the cycling progressed. However, the extent of crack formation was reduced by the Nafion coating layer. Because the Young's modulus and yield strength of the Nafion layer tend to increase with the ionic radii of metal ions (such as Li^+ Na^+ K^+, Cs^+, and Rb^+) [24,26,27], this layer suppresses crack formation due to interaction with the lithium ions in the electrolyte. ICP-MS was used to quantitatively analyze the vanadium dissolution in the electrolyte after the 100th cycle (Fig. 7). As shown in Fig. 7, the dissolved vanadium amount detected in the Nafion coated LiV_3O_8-containing cell was much lesser: vanadium content in the electrolyte was 350–670 ppb in the bare LiV_3O_8-containing cell, whereas it was only 75–85 ppb in the Nafion coated LiV_3O_8-containing cell, which was approximately one-seventh of the vanadium content of the uncoated cell. Thus, the Nafion coating layer blocked direct contact between the electrode and the electrolyte, thus suppressing vanadium dissolution. These two effects caused by the coating improved the electrochemical performance of the Nafion coated LiV_3O_8 electrode.

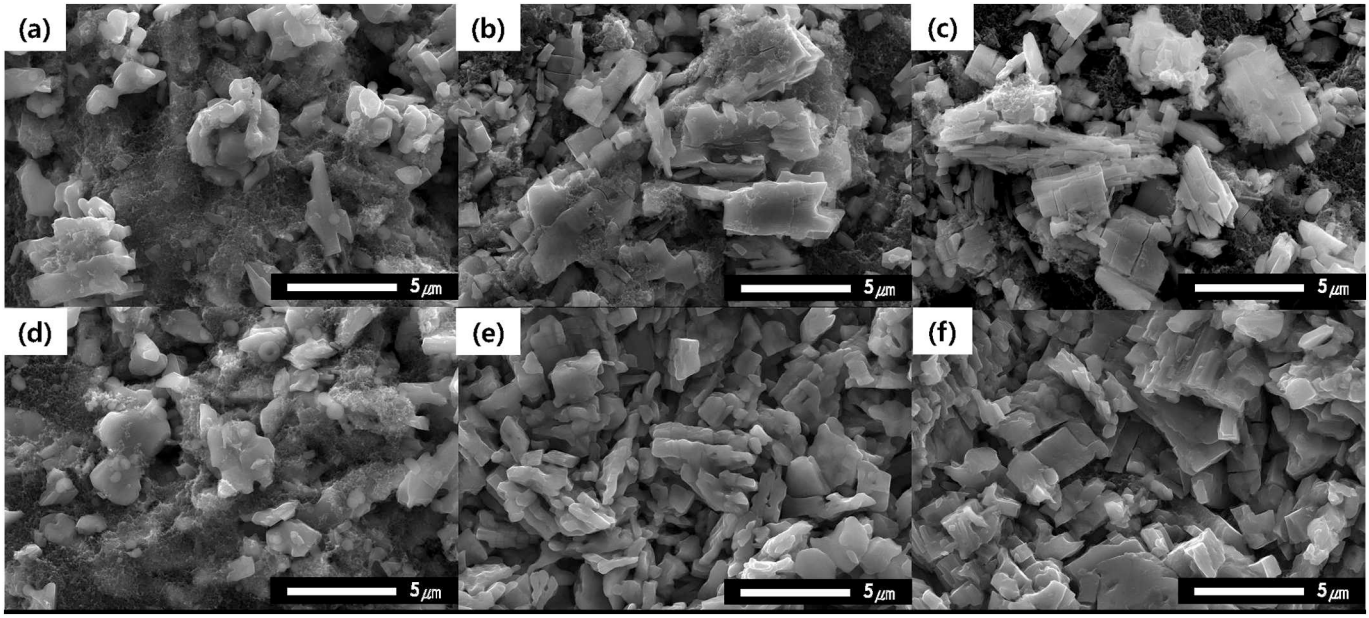

Fig. 6. (a)–(f) SEM images of bare and Nafion coated LiV_3O_8 electrodes and their surface morphological variation in the 1st, 100th, and 200th cycle.

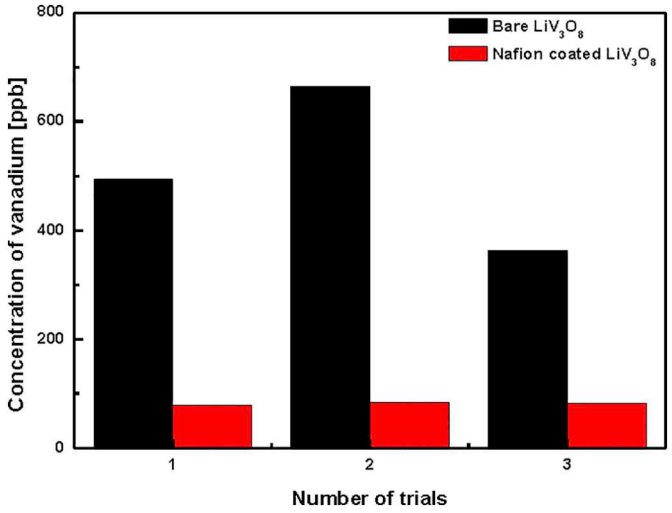

Fig. 7. Vanadium dissolution in the electrolyte after the 100th cycle for bare LiV_3O_8-containing (Black) and Nafion coated LiV_3O_8-containing cells (Red). (For interpretation of the references to color in this figure legend, the reader is referred to the web version of this article.)

Fig. 8(a) shows the impedance analysis results for the bare and Nafion coated LiV_3O_8 electrodes and the equivalent circuit. Table 2 lists the impedance fitting data. A Randles circuit was used to demonstrate the electrochemical reaction occurring on the surface of the bare and Nafion coated LiV_3O_8 electrodes. In this equivalent circuit, R_s is the sum of ohmic resistance of the electrode and electrolyte and R_{ct} is the charge-transfer resistance in parallel in the Randles circuit; this circuit provides information concerning the electrical conductivity, crystal structure, interparticle contact, and surface condition of the electrode. A constant phase element (CPE1) related to R_{ct} results in the inclusion of a small semicircle in the corresponding Nyquist plot. W_1 is associated with the Li^+ diffusion resistance in the electrode [40–44]. As shown in Fig. 8(a) and Table 2, the R_s and R_{ct} values of the Nafion coated LiV_3O_8 electrode were lower than those of the bare LiV_3O_8 electrode. Due to lower R_{ct}, the Nafion coated LiV_3O_8 electrode showed improved electrochemical performance and enhanced cycling characteristics. Fig. 8(b) shows the fitted line for Z_{re} vs. $\omega^{-1/2}$, from which the graph could be derived, and the Li^+ diffusion coefficient (D) was calculated using Eq. (1):

$$D = 0.5\,(RT/An^2F^2\sigma_\omega C)^2 \quad (1)$$

Here, R is the gas constant, T is the temperature, A is the effective contact area between the electrode and the electrolyte, n is the number of electrons transferred per mole of the active material involved in the electrode reaction, F is the Faraday constant, and C is the concentration of Li^+ in the cathode based on the crystallographic cell parameters of LiV_3O_8 [45]. The $D_{Li}{}^+$ value of the Nafion coated LiV_3O_8 electrode ($\sigma_\omega = 3.222\,\Omega{\cdot}s^{-1/2}$) was $2.08 \times 10^{-13}\,cm^2{\cdot}S^{-1}$, indicating its better Li^+ diffusion ability than the bare LiV_3O_8 electrode ($9.60 \times 10^{-14}\,cm^2{\cdot}S^{-1}$). In other words, the coating layer assisted Li^+ diffusion and electron transportation, thereby leading to a low value for R_{ct} and high value for the lithium diffusion coefficient in the Nafion coated electrode [23,46,47].

4. Conclusion

LiV_3O_8 was synthesized by a solid-state method and Nafion was uniformly coated on the electrode surface using electrostatic spray deposition. Electrostatic spray deposition is an effective technique to coat an inert polymer such as Nafion on the electrode. A cell assembled using the Nafion coated LiV_3O_8 cathode and a powdered lithium metal anode showed a higher discharge capacity over diverse C rates and better capacity retention ($150.86\,mAh\,g^{-1}$ and 62.9%, respectively) even after 200 cycles than a cell assembled using the bare LiV_3O_8 cathode ($113.31\,mAh\,g^{-1}$ and 46.8%, respectively). This enhanced electrochemical performance was ascribed to the Nafion coating, which not only acted as a buffer layer against volume expansion but also prevented direct contact between the electrode and the electrolyte. Also, a proper coating method such as electrostatic spray deposition was needed to guarantee the physical and chemical soundness of the coating layer. Furthermore, the Nafion coated LiV_3O_8 electrode exhibited a low charge-transfer resistance, which indicated improved

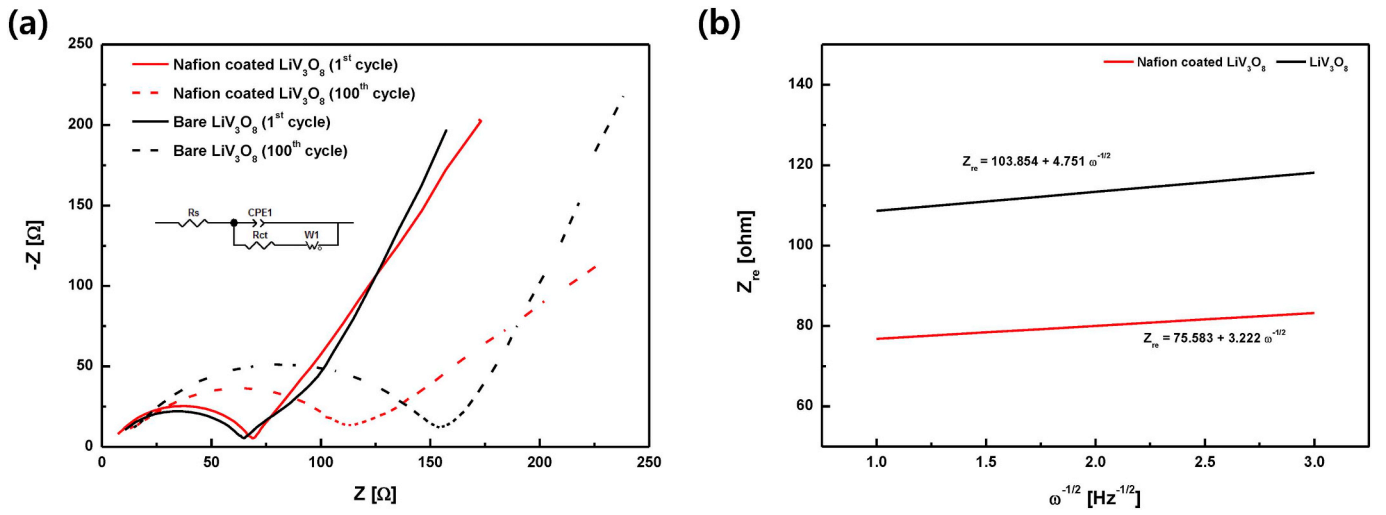

Fig. 8. (a) Results of impedance analysis of LiV_3O_8 and Nafion coated LiV_3O_8 electrodes and equivalent circuit for calculating impedance results and (b) fitted line for Z_{re} vs. $\omega^{-1/2}$, which was used to obtain impedance data.

Table 2
Impedance fitting data of bare and Nafion coated LiV_3O_8 electrodes.

	LVO		Nafion coated LiV_3O_8	
	1st cycle	100th cycle	1st cycle	100th cycle
Rs [Ω]	7.544	9.164	3.553	5.124
Rct [Ω]	96.31	152.3	70.03	124.2
W [$\Omega^{-1}\cdot S^{1/2}\cdot cm^{-2}$]	4.751	3.308	3.222	3.277
D_{Li^+}	9.6×10^{-14}	1.98×10^{-13}	2.08×10^{-13}	2.02×10^{-13}

electrical conductivity and rapid lithium-ion migration. Therefore, these results suggested that Nafion coated LiV_3O_8 electrodes are promising cathode materials for lithium-metal rechargeable batteries.

Acknowledgements

This study was supported by a National Research Foundation of Korea (NRF) grant, funded by the Korean Government (MEST, 2016R1A2B3009481). TEM examination was performed at the Korea Basic Science Institute, Seoul Center.

References

[1] B. Dunn, H. Kamath, J.-M. Tarascon, Electrical energy storage for the grid: a battery of choices, Science 334 (2011) 928–935.
[2] K.C. Divya, J. Østergaard, Battery energy storage technology for power systems—an overview, Electr. Power Syst. Res. 79 (2009) 511–520.
[3] M. Mori, Y. Naruoka, K. Naoi, Modification of the lithium metal surface by nonionic polyether surfactants: quartz crystal microbalance studies, J. Electrochem. Soc. 145 (1998) 2340–2348.
[4] D. Aurbach, E. Zinigrad, Y. Cohen, H. Teller, A short review of failure mechanisms of lithium metal and lithiated graphite anodes in liquid electrolyte solutions, Solid State Ionics 148 (2002) 405–416.
[5] J.-S. Kim, W.-Y. Yoon, B.-K. Kim, Morphological differences between lithium powder and lithium foil electrode during discharge/charge, J. Power Sources 163 (2006) 258–263.
[6] J.S. Kim, W.Y. Yoon, K.Y. Yi, B.K. Kim, B.W. Cho, The dissolution and deposition behavior in lithium powder electrode, J. Power Sources 165 (2007) 620–624.
[7] I.W. Seong, C.H. Hong, B.K. Kim, W.Y. Yoon, The effects of current density and amount of discharge on dendrite formation in the lithium powder anode electrode, J. Power Sources 178 (2008) 769–773.
[8] J.S. Kim, S. hoon Baek, W.Y. Yoon, Electrochemical behavior of compacted lithium powder electrode in Li/V_2O_5 rechargeable battery, J. Electrochem. Soc. 157 (2010) A984–A987.
[9] S.-K. Kong, B.-K. Kim, W.-Y. Yoon, Electrochemical behavior of Li-powder anode in high Li capacity used, J. Electrochem. Soc. 157 (2012) A1551–A1553.
[10] J.-M. Tarascon, M. Armand, Issues and challenges facing rechargeable lithium batteries, Nature 414 (2001) 359–367.
[11] J.-S. Lee, S.T. Kim, R. Cao, N.-S. Choi, M. Liu, K.T. Lee, J. Cho, Metal–air batteries with high energy density: Li–air versus Zn–air, Adv. Energy Mater. 1 (2011) 34–50.
[12] M.A. Rahman, X. Wang, C. Wen, High energy density metal-air batteries: a review, J. Electrochem. Soc. 160 (2013) A1759–A1771.
[13] P.G. Bruce, S.A. Freunberger, L.J. Hardwick, J.-M. Tarascon, Li–O2 and Li–S batteries with high energy storage, Nat. Mater. 11 (2012) 19–29.
[14] S. Evers, L.F. Nazar, New approaches for high energy density lithium-sulfur battery cathodes, Acc. Chem. Res. 46 (2013) 1135–1143.
[15] L. Jiao, L. Liu, J. Sun, L. Yang, Y. Zhang, H. Yuan, Y. Wang, X. Zhou, Effect of $AlPO_4$ nanowire coating on the electrochemical properties of LiV_3O_8 cathode material, J. Phys. Chem. C 112 (2008) 18249–18254.
[16] W. Ren, Z. Zheng, Y. Luo, W. Chen, C. Niu, K. Zhao, M. Yan, L. Zhang, J. Meng, L. Mai, An electrospun hierarchical LiV_3O_8 nanowire-in-network for high-rate and long-life lithium batteries, J. Mater. Chem. A 3 (2015) 19850–19856.
[17] S.Y. Chew, C. Feng, S.H. Ng, J. Wang, Z. Guo, H. Liu, Low-temperature synthesis of polypyrrole-coated LiV_3O_8 composite with enhanced electrochemical properties, J. Electrochem. Soc. 154 (2007) A633–A637.
[18] Y. Feng, Y. Li, F. Hou, Preparation and electrochemical properties of Cr doped LiV_3O_8 cathode for lithium ion batteries, Mater. Lett. 63 (2009) 1338–1340.
[19] A. Pan, J.-G. Zhang, G. Cao, S. Liang, C. Wang, Z. Nie, B.W. Arey, W. Xu, D. Liu, J. Xiao, G. Li, J. Liu, Nanosheet-structured LiV_3O_8 with high capacity and excellent stability for high energy lithium batteries, J. Mater. Chem. 21 (2011) 10077–10084.
[20] X. Ren, S. Hu, C. Shi, P. Zhang, Q. Yuan, J. Liu, Preparation and electrochemical properties of Zr-doped LiV_3O_8 cathode materials for lithium-ion batteries, J. Solid State Electrochem. 16 (2012) 2135–2141.
[21] H. Song, Y. Liu, C. Zhang, C. Liu, G. Cao, Mo-doped LiV_3O_8 nanorod-assembled nanosheets as a high performance cathode material for lithium ion batteries, J. Mater. Chem. A 3 (2015) 3547–3558.
[22] X.-W. Gao, J.-Z. Wang, S.-L. Chou, H.-K. Liu, Synthesis and electrochemical performance of LiV_3O_8/polyaniline as cathode material for the lithium battery, J. Power Sources 220 (2012) 47–53.
[23] S. Huang, J.P. Tu, X.M. Jian, Y. Lu, S.J. Shi, X.Y. Zhao, T.Q. Wang, X.L. Wang, C.D. Gu, Enhanced electrochemical properties of Al_2O_3-coated LiV_3O_8 cathode materials for high-power lithium-ion batteries, J. Power Sources 245 (2014) 698–705.
[24] S.C. Yeo, A. Eisenberg, Physical properties and supermolecular structure of perfluorinated ion-containing (Nafion) polymers, J. Appl. Polym. Sci. 21 (1977) 875–898.
[25] M.A. Harmer, W.E. Farneth, Q. Sun, High surface area Nafion† resin/silica nanocomposites: a new class of solid acid catalyst, J. Am. Chem. Soc. 118 (1996) 7708–7715.
[26] M. Doyle, S.K. Choi, G. Proulx, High-temperature proton conducting membranes based on perfluorinated ionomer membrane-ionic liquid composites, J. Electrochem. Soc. 147 (2000) 34–37.
[27] S. Kundu, L.C. Simon, M. Fowler, S. Grot, Mechanical properties of Nafion™ electrolyte membranes under hydrated conditions, Polymer 46 (2005) 11707–11715.
[28] Z. Jin, K. Xie, X. Hong, Z. Hu, X. Liu, Application of lithiated Nafion ionomer film as functional separator for lithium sulfur cells, J. Power Sources 218 (2012) 163–167.
[29] Q. Tang, Z. Shan, L. Wang, X. Qin, K. Zhu, J. Tian, X. Liu, Nafion coated sulfur–carbon electrode for high performance lithium–sulfur batteries, J. Power Sources 246 (2014) 253–259.
[30] C.M. Ghimbeu, R.C. van Landschoot, J. Schoonman, M. Lumbreras, Tungsten trioxide thin films prepared by electrostatic spray deposition technique, Thin Solid Films 515 (2007) 5498–5504.
[31] H. Yoon, M.G. Malia, M.W. Kim, S.S. Al-Deyab, S.S. Yoon, Electrostatic spray deposition of transparent tungsten oxide thin-film photoanodes for solar water

splitting, Catal. Today 260 (2016) 89–94.
[32] S.H. Cho, S.W. Hwang, B.H. Kim, K.Y. Bae, H. Yoon, S.S. Yoon, W.Y. Yoon, Electrochemical properties of Li metal batteries with P(PEGMA)-coated lithium trivanadate cathode and Li powder anode, J. Nanosci. Nanotechnol. 16 (2016) 10607–10612.
[33] A. Pan, J. Liu, J.-G. Zhang, G. Cao, W. Xu, Z. Nie, X. Jie, D. Choi, B.W. Arey, C. Wang, S. Liang, Template free synthesis of LiV_3O_8 nanorods as a cathode material for high-rate secondary lithium batteries, J. Mater. Chem. 21 (2011) 1153–1161.
[34] A. Caballero, J. Morales, O.A. Vargas, Electrochemical instability of LiV_3O_8 as an electrode material for aqueous rechargeable lithium batteries, J. Power Sources 195 (2010) 4318–4321.
[35] X. Xu, Y.-Z. Luo, L.-Q. Mai, Y.-L. Zhao, Q.-Y. An, L. Xu, F. Hu, L. Zhang, Q.-J. Zhang, Topotactically synthesized ultralong LiV_3O_8 nanowire cathode materials for high-rate and long-life rechargeable lithium batteries, NPG Asia Mater. 20 (2012) 1–7.
[36] G. Yang, W. Hou, Z. Sun, Q. Yan, A novel inorganic–organic polymer electrolyte with a high conductivity: insertion of poly(ethylene) oxide into LiV_3O_8 in one step, J. Mater. Chem. 15 (2005) 1369–1374.
[37] S.J. Oh, J.K. Lee, W.Y. Yoon, Preventing the dissolution of lithium polysulfides in lithium–sulfur cells by using Nafion-coated cathodes, ChemSusChem 7 (2017) 2562–2566.
[38] M. Dekam, A. Kumar, Enhanced ionic conductivity in novel nanocomposite gel polymer electrolyte based on intercalation of PMMA into layered LiV_3O_8, J. Solid State Electrochem. 14 (2010) 1649–1656.
[39] N.H. Idris, M.M. Rahman, J.-Z. Wang, Z.-X. Chen, H.-K. Liu, Synthesis and electrochemical performance of LiV_3O_8/carbon nanosheet composite as cathode material for lithium-ion batteries, Compos. Sci. Technol. 71 (2011) 343–349.
[40] S. Shiraishi, K. Kanamura, Z. Takehara, Surface condition changes in lithium metal deposited in nonaqueous electrolyte containing HF by dissolution-deposition cycles, J. Electrochem. Soc. 146 (1999) 1633–1639.
[41] P. Xiao, Y. Zhang, B.B. Garcia, S. Sepehri, D. Liu, G. Cao, Nanostructured electrode with titania nanotube arrays: fabrication, electrochemical properties, and applications for biosensing, J. Nanosci. Nanotechnol. 9 (2009) 2426–2436.
[42] N.N. Sinha, N. Munichandraiah, Synthesis and characterization of carbon-coated LiNi1/3Co1/3Mn1/3O2 in a single step by an inverse microemulsion route, ACS Appl. Mater. Interfaces 1 (2009) 1241–1249.
[43] Y.Q. Qiao, J.P. Tu, X.L. Wang, J. Zhang, Y.X. Yu, C.D. Gu, Self-assembled synthesis of hierarchical waferlike porous Li-V-O composites as cathode materials for lithium ion batteries, J. Phys. Chem. C 115 (2011) 25508–25518.
[44] Z.-K. Wang, J. Shu, Q.-C. Zhu, B.-Y. Cao, H. Chen, X.-Y. Wu, B.M. Bartlett, K.-X. Wang, J.-S. Chen, Graphene-nanosheet-wrapped LiV_3O_8 nanocomposites as high performance cathode materials for rechargeable lithium-ion batteries, J. Power Sources 307 (2016) 426–434.
[45] W. Li, L. Zhu, Z. Yu, L. Xie, X. Cao, LiV_3O_8/polytriphenylamine composites with enhanced electrochemical performances as cathode materials for rechargeable lithium batteries, Materials 10 (2017) 1–13.
[46] A.J. Bard, L.R. Faulkner, Electrochemical Methods, second ed., John Wiley & Sons, New York, 2001, p. 231.
[47] A.Y. Shenouda, H.K. Liu, Electrochemical behavior of tin borophosphate negative electrodes for energy storage systems, J. Power Sources 185 (2008) 1386–1391.